Integration, Alignment, and Initial Performance Results of the *Far Ultraviolet Spectroscopic Explorer* (FUSE) Spectrograph

Erik Wilkinson[a], James C. Green[a], Steven N. Osterman[a]
Kenneth R. Brownsberger[a], & David J. Sahnow[b]

[a]Center for Astrophysics and Space Astronomy
University of Colorado, Boulder, CO 80309

[b]Department of Physics and Astronomy
Johns Hopkins University, Baltimore, MD 21218

1. ABSTRACT

The Center for Astrophysics and Space Astronomy (CASA) recently delivered to the Johns Hopkins University the Far Ultraviolet Spectrograph instrument for integration into the Far Ultraviolet Spectroscopic Explorer (FUSE) satellite. In addition to the optical design of the FUSE instrument, the CASA/FUSE team was responsible for development of major optical components of the spectrograph and the final assembly and alignment of the instrument. In this paper we present the optical design, alignment methodologies employed, and performance characteristics of the instrument as delivered to the Johns Hopkins University. In addition, we discuss how we determined the resolution of the instrument and the difficulties in determining the resolving power when working with an FUV instrument capable of resolving powers in excess of 30,000. We also discuss the contamination control and monitoring and stability testing of the instrument, i.e. vibration, thermal distortion, and long term (12 hour) stability testing.

Keywords: spectrograph, space, ultraviolet, high resolution, FUSE

2. INTRODUCTION

2.1 FUSE scientific mission

The Far Ultraviolet Spectroscopic Explorer (FUSE) is a NASA astronomy mission dedicated to making high resolution ($\lambda/\Delta\lambda$ = 20,000 to 30,000), high sensitivity (Aeff = 20–70 cm^2). spectroscopic. observations. between. 900.. and. 1190.. FUSE is currently scheduled for launch in early 1999 on a Delta II launch vehicle and will conduct a wide range of scientific observing programs over a 3 year mission lifetime. The combined high resolution, high throughput design of FUSE will provide the scientific community with a unique opportunity to address such scientific issues as the distribution of hot gas in the galaxy, the dynamics and structure of the stellar atmospheres, and the abundance.s of primordial gases in the intergalactic medium to mention just a few[1,2].

2.2 The FUSE instrument

The FUSE instrument consists of 4 spectroscopic channels which share 2 detector systems. Collimated light is collected by 4 off–axis parabolic telescopes with 2245 mm focal lengths. Two of the telescopes are coated with silicon. carbide. (SiC). to. optimize. the. effective. area. below. 1050.... The. remaining. two. telescopes. are. coated. with aluminum/lithium fluoride. (Al/LiF). to. maximize. the. effective. area. above. 1050.... The. light. from. a telescope is focused onto one of four entrance apertures and is then diffracted a large, holographically ruled, spherical grating[2,3,4]. The diffracted light then focuses onto a double delay line microchannel plate (MCP) detector[5]. The microchannel plates are coated with a potassium bromide (KBr) photocathode to optimize the detection quantum efficiency in the FUSE bandpass.

The overall instrument length is 4 meters and is assembled onto a two piece, graphite epoxy structure. The lower half of the structure contains the parabolic telescopes and the instrument electronics. The upper half of the structure is the far ultraviolet spectrograph (FUVS) and houses the entrance slits, gratings, baffles, and detectors.

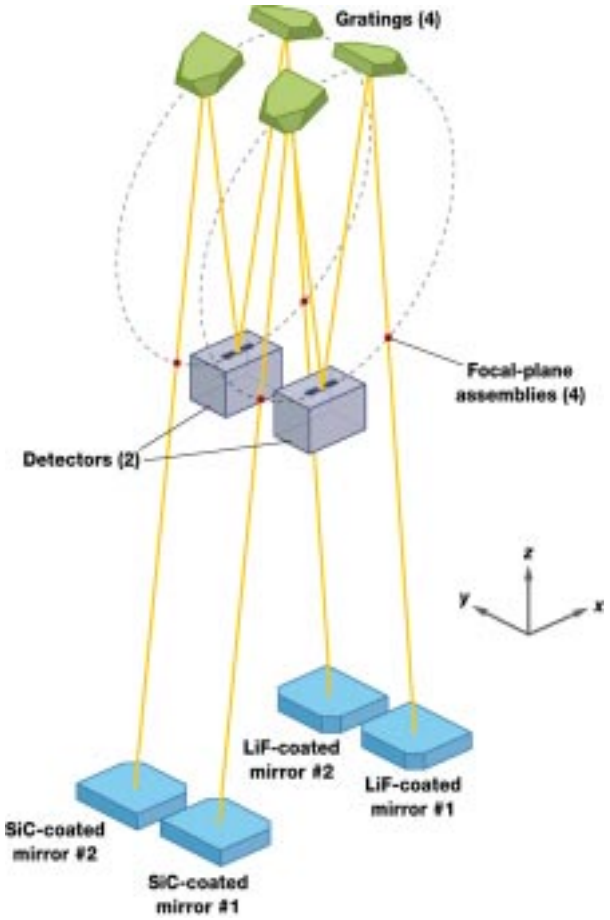
Gratings (4)
Focal-plane assemblies (4)
Detectors (2)
z
y
x
LiF-coated mirror #2
LiF-coated mirror #1
SiC-coated mirror #2
SiC-coated mirror #1

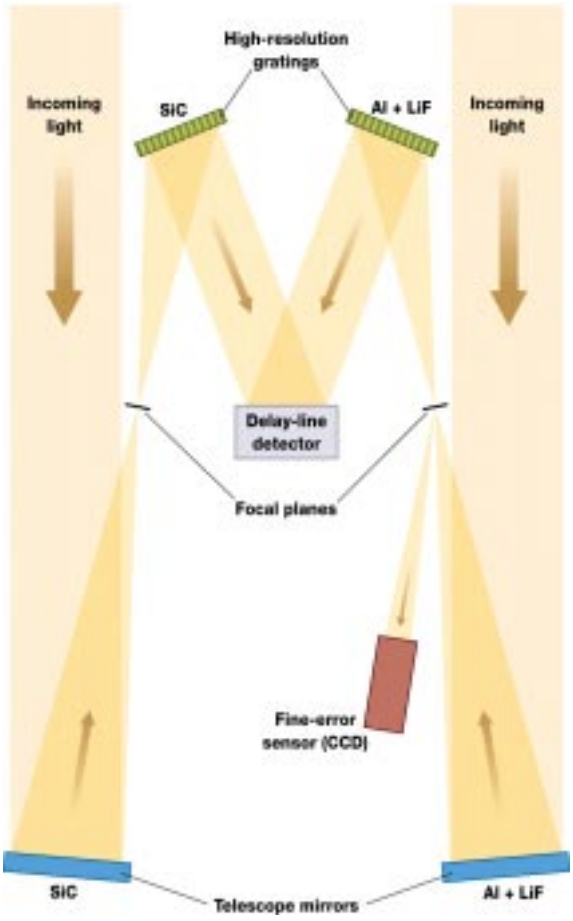

(a) (b)

Figure 1: (a) Schematic drawing of the FUSE instrument showing the four optical paths and two detectors. (b) Shows how the light enters one pair of channels and is diffracted onto the double delay line detector.

3. THE FAR ULTRAVIOLET SPECTROGRAPH (FUVS)

3.1 Optical design

The FUVS has four spectrograph channels which share 2 double delay line, microchannel plate detectors[5]. Each channel is conceptually similar to a Rowland circle spectrograph, except that aberration corrected, holographically ruled gratings are used to control the astigmatism typically encountered in a Rowland system[4,6,7]. The gratings are paired so that a single detector has spectra from both a SiC and a LiF grating. The Rowland circle diameters are 1652 mm with the SiC coated gratings having a characteristic ruling density of 5767 grooves/mm and the LiF coated gratings having 5400 grooves/mm... Therefore,. the. SiC. channel. has. a. 1.03../mm. disperson. and. the. LiF channel. has. a. 1.12../mm. disperson.

For each spectrograph channel light from the off-axis parabolic telescope enters the spectrograph through a Focal Plane Assembly (FPA)[8]. Each FPA has four laser drilled entrance apertures;. 1.25.. X. 20.,. 4.. X. 20.,. 30.. X. 30.,. and. a 0.5.. pinhole... The. front. surface. of. each. FPA. is. a. diamond. milled,. flat. mirror. with. vapor. deposited. aluminum. to provide a highly reflective surface in the visible. Light which does not pass through an entrance aperture is reflected into the Fine Error Sensor (FES), which provides feedback to the spacecraft attitude control system for

stabilizing the pointing. Only the LiF channels are equipped with FES systems, because the Al/LiF coatings on the telescopes are far more reflective in the visible than the SiC coatings.

The diverging f/5.3 beam passes into the spectrograph cavity where it encounters one of the gratings. Each FUVS grating consists of a rectangular fused silica substrate 270 mm X 265 mm on a side with concave, spherical surface with a 1652±1 mm radius of curvature and holographically recorded diffraction rulings[9]. In the case of FUSE, the gratings are first generation, type 1 holographic gratings[4,6,7]. The holographic recording parameters were optimized to reduce the astigmatism from approximately 60 mm (using standard parallel groove gratings) to less than 1 mm while maintaining 30,000 resolution. This dramatically increases the sensitivity of the instrument.

The diffracted light then focuses onto the double delay line, microchannel plate detectors. Each detector has an active area of 190 mm X 10 mm which is divided into two 85 mm X 10 mm MCP stacks, referred to as the A segment and the B segment. The microchannel plates are curved to 826 ±1 mm and a potassium bromide (KBr) photocathode is applied to the top MCP plates to enhance the detection quantum efficiency in the FUV[5]. The average resolution of the FUSE detectors is 25 μm in the spectral direction and 50–60 μm in the spatial dimension.

4. INTEGRATION AND COARSE ALIGNMENT

4.1 Alignment algorithm

Using raytrace models we developed an alignment algorithm for use during the FUV alignment. This algorithm was a two step process in which the gratings were first tipped and tilted to position the ArI 1048 and 1066 lines at their design location on the detector. The FPAs were then pistoned along the incident light path to focus the emission lines. Based on this methodology and inputs from the engineers designing the vacuum manipulation mechanisms, an error budget for the installation of the optical components was developed. This error budget was very simple, requiring that each optical component be positioned to within ±1 mm and ±1 arcminute of its design location with respect to the detector focal plane surface.

4.2 Coarse alignment

The large physical size of the instrument made theodolite metrology an attractive technology for meeting the installation tolerances. Theodolite metrology uses 2 or more class 1 theodolites and an accurate length standard to develop a known coordinate system with respect to the theodolites. Once the system is calibrated, then the position of any point can be measured in the three dimensional theodolite coordinate system. The accuracy of the theodolite metrology systems now available are on order 0.002 to 0.005 . Thus, such a system is quite capable of meeting the FUVS installation and coarse alignment requirements.

In order to position the optical components accurately, it is necessary to be able to either directly view the surface being aligned or use an external reference which has a known orientation with respect to the primary surface. In the case of the FUVS, it was not easy to view the critical surfaces, therefore we used optical cubes and alignment targets to form secondary references to coarsely align the components.

All components were installed with respect to the instrument prime coordinate system (IPCS). Ten adhesive targets were installed onto the flight structure and their positions in IPCS were measured. These targets were then used to quickly reorient the theodolite based coordinate system into IPCS during component coarse alignment and position monitoring. The rotational datum for aligning the gratings in rotation were optical cubes mounted onto each detector.

Each grating mount assembly (GMA) had an optical cube bonded to the back of the grating. The cube also had a cross hair target etched on one face which formed the translational datum. The cube's rotational and translational orientation with respect to the grating was calibrated using the theodolite metrology system prior to installation

on the structure. The face of the slit mirrors on each FPA were inaccessible for coarse alignment. Therefore, each FPA had adhesive aluminum targets attached in two places. The orientation of the targets with respect to the entrance apertures and the normal of the slit mirror were calibrated prior to installation onto the structure.

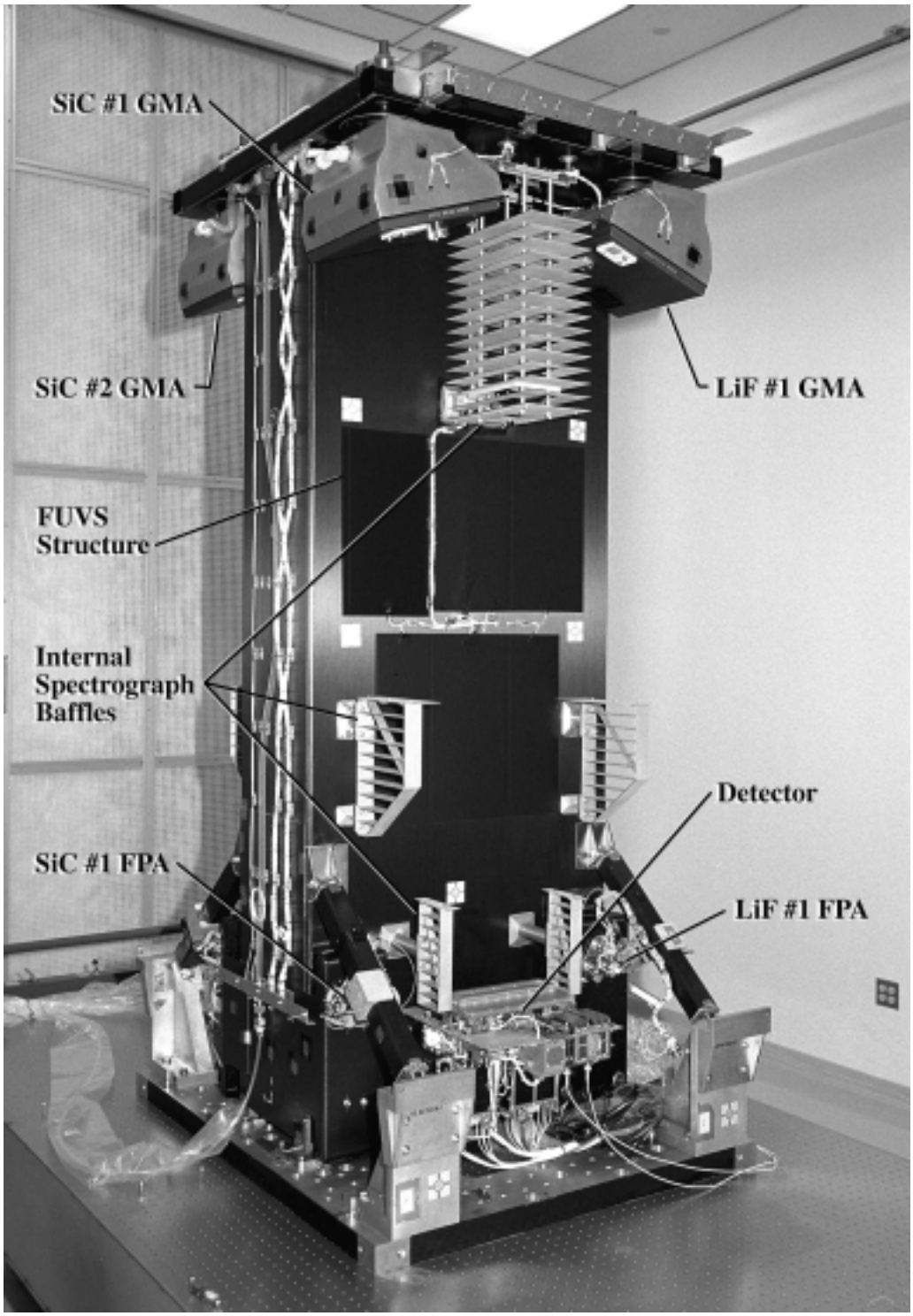

Figure 2: Photograph of the FUVS just prior to shipment to Johns Hopkins University with the major optical components identified

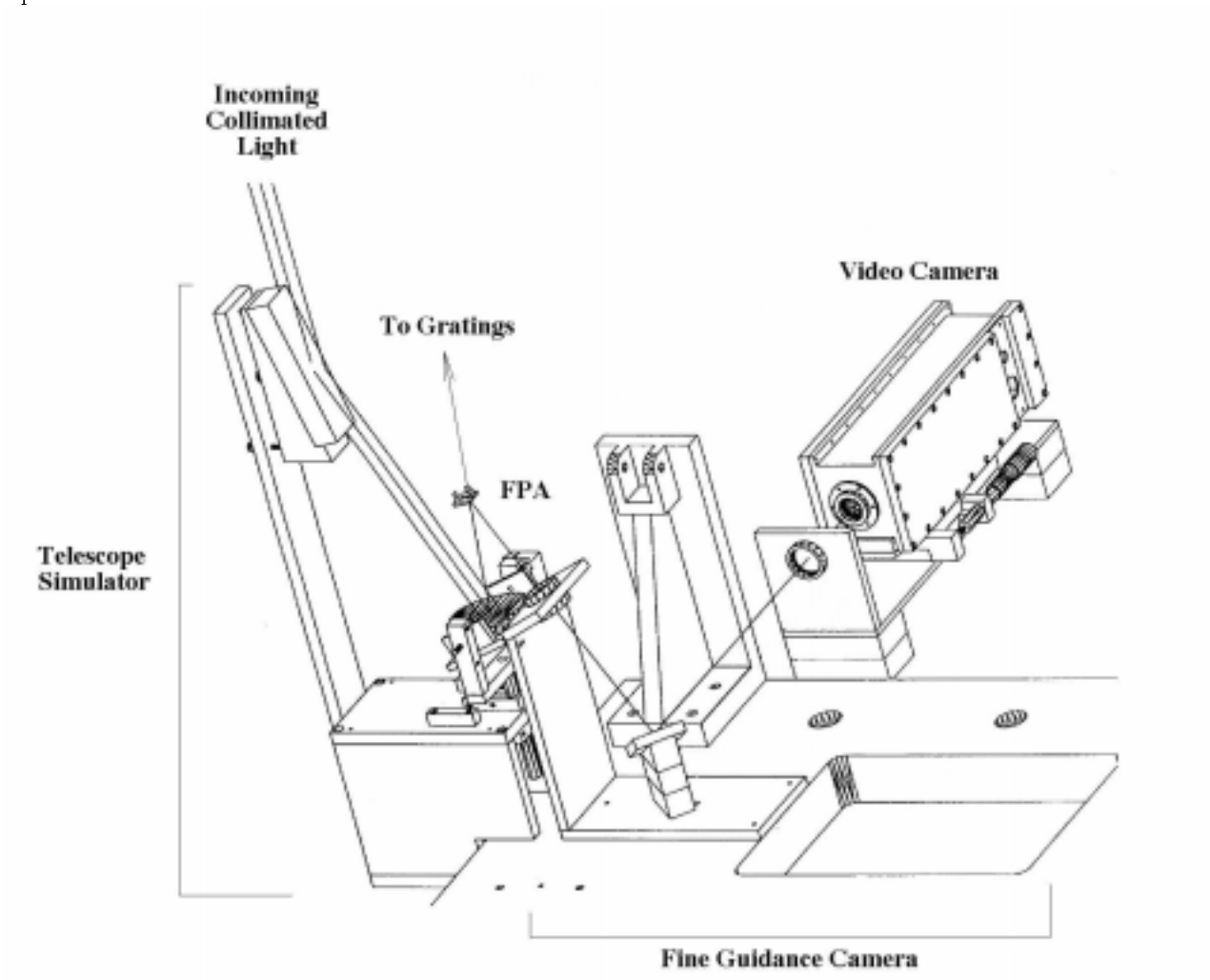

Figure 3 : Schematic showing the optical ground support equipment around the FPA. Collimated light is redirected and then focused by the telescope simulator. The telescope simulator produces a cone of light of the same speed and direction as that produced by the flight telescopes. Light which does not pass through the entrance slits at the FPA is redirected and then reimaged by the fine guidance camera. The fine guidance camera consists of a two lens, one mirror optical system which reimages the light from the FPA onto a video camera. The images from the video camera provide feedback on where the light is on the flight slit.

5. FINE ALIGNMENT

5.1 Optical GSE

The absence of an optical material which can transmit radiation below about 1050 Å, the short wavelength cut-off of LiF crystals, necessitated that the precision alignment of the FUVS be done using far ultraviolet radiation (900 to 1200 Å) in a high vacuum environment... Therefore, we had to develop a significant amount of optical ground

support equipment (OGSE) to enable us to introduce FUV radiation into a vacuum chamber, manipulate it, and to simulate the telescope beam.

The OGSE light path consisted first of a 90° off axis parabolic collimator which resided outside of the vacuum tank along with the flowing gas discharge light sources and associated support hardware. Light from the discharge sources was introduced through a pinhole located at the focus of the parabolic collimator. Gatevalves were used to isolate the collimator and light sources from the main chamber when the sources were not in use. When the valves were open the collimated beam was introduced into the main chamber. The collimated beam was intercepted by a telescope simulator mounted to the same optical bench as the FUVS. The telescope simulator consisted of two optics; a flat transfer mirror and a 30ø off axis parabolic mirror (see figure 3). This combination produced a converging cone of light with an incident angle and beam speed similar to that produced by the flight telescopes (90% encircled energy in 1.5 arcseconds). However, the imaging quality and scatter of the OGSE was far inferior to the flight telescopes. The result of this choice was that the 1.25 arcsecond slit used during spectrograph focusing was fully illuminated in the spectral direction. This was done to minimize the cost and schedule requirements of the OGSE.

Light that did not pass through the flight slits at the focus of the telescope simulators was reflected by the mirrored region around the slits and reimaged by a two lens, one mirror optical train onto a standard CCD camera. The CCD camera provided optical feedback during alignment of the image onto the flight slits during testing and alignment. While at vacuum, adjustments to the image location on the slits were accomplished using external micrometers to adjust the pinhole at the collimator focus and thus move the image at the FPA mirror and through translation of the telescope simulator itself using vacuum rated micropositioning hardware.

5.2 Opto-mechanical GSE

Since the precision alignment of the FUVS had to be done in vacuum, we needed a means of manipulating the flight optics during vacuum operations. The FPAs were mounted to a 2 axis (x and z in IPCS, see figure 1) manipulation stage with micron level accuracy. This allowed us to move each FPA along the incident light ray during the focusing process. The GMAs were provided with tip, tilt, and rotation about the IPCS z axis. This allowed remote adjustment of the grating orientation to position the spectrum in the spectral and spatial dimensions on the detector with an accuracy of about 10 arcseconds[9]. Both of these opto-mechanical GSE systems were controlled via computer interfaces in the main control area of the integration and test control center.

6. FUVS PERFORMANCE

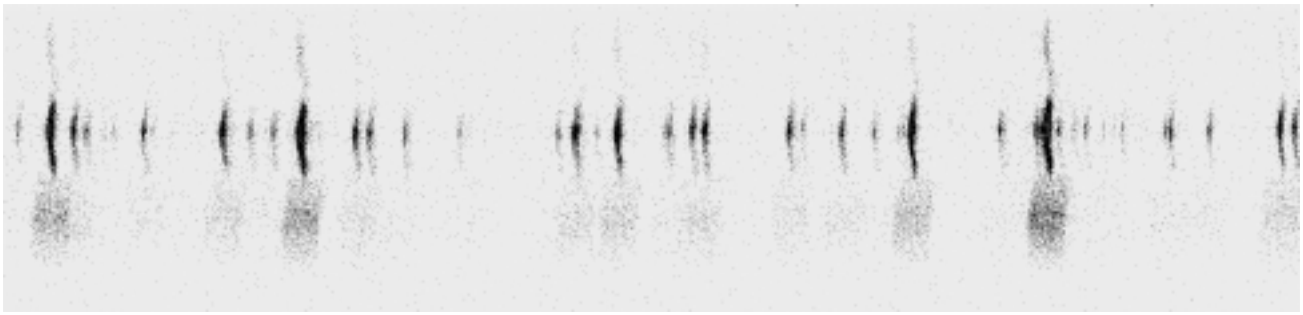

Figure 4: LiF#1 spectrum of Pt/Ne. Clearly evident are the images of the 3 flight slits. The middle and most prominent. spectrum. uses. the. 1.25.. slit,. the. spectrum. at. the. top. of. the. figure. is. formed. by. scattered. light. through the. 4.. slit. and. the. bottom. spectrum. is. formed. by. scattered. light. through. the. 30.. slit.

6.1 Wavelength coverage

In the table below we list the wavelength coverage.s of each spectrograph channel. Except for wavelengths between 1082.2.. and. 1085.6.,. all. wavelengths. from. 916.8.. through. 1181.7.. are. covered. by. at. least. two. channels.

	Detector Segment	
Channel	A	B
SiC#1	1091.1. –. 1003.9.	992.6. –. 905.0.
SiC#2	916.8. –. 1006.4.	1016.3. –. 1105.0.
LiF#1	987.1 – 1082.2.	1094.3 – 1187.7.
LiF#2	1181.7. –. 1085.6.	1074.6. –. 978.1.

6.2 Resolution

The resolution curves for the FUVS channels are presented in figure 6. Resolution in this case is defined at $\lambda/\Delta\lambda$ where $\Delta\lambda$ is the fwhm of the line multiplied by the dispersion. The resolution of a given line is a function of the entrance slit width, the natural width of the emission line being used, the grating imaging performance, and the detector performance.

The point spread function (psf) of the flight telescopes is far superior to the psf produced by the OGSE. Therefore, we expect a modest improvement in the resolution on the order of 2000 in flight compared to the ground performance. The detector performance, on the other hand, has profound impact on the resolution. As delivered the resolution of each detector segment varies from about 30–40 μm at the edges to about 20 μm in the middle in a smoothly varying function. Detector resolutions above 25 μm begin to decrease the instrument resolution quickly. Therefore, if the instrument resolution were detector limited the resolution curve should peak towards the middle of a detector segment with lower resolutions at the segment edges. However, this effect would only be evident if the detector was the primary limiting factor in the resolution.

In our initial attempts to focus the FUVS LiF#1 channel we investigated Ar, N_2, O_2, CO, Pt/Ne, H_2, and a H/D mix as sources of line emission in our flowing gas discharge lamps. We found eventually that the Ar, N_2, and O_2 were useless for focusing as the widths of the emission lines produced by our sources were far too broad. CO has one molecular complex near. 1150.. that. was. useful for focusing. The Pt/Ne hollow cathode lamps with a LiF window provided very narrow lines, but the source was too dim for efficient focusing and only covered the long wavelength segment of the LiF channels. H_2 or H/D were the most useful gases, having narrow lines across the full wavelength bandpass of the FUVS. The down side was that H_2 produced hundreds of lines with only a few lines narrow enough to actually focus the instrument.

To confront the H_2 problem, we developed a technique for focusing. we. called. the. .shotgun.. method... In. the. shotgun method we would fit *e v e r y* emission line we could find and then plot the line width versus detector x pixel. The idea is that the naturally narrow lines will define the best resolution, i.e. the lower edge of the line widths versus x pixel number distribution. This technique worked quite well in general and we were able to focus the instrument using H_2. While this technique did allow us to identify the best focus position, the absolute value of the resolution curves came into question.

6.2.1 LiF#1 and LiF#2 resolution

The LiF channels were fairly easy to align and as shown in figure 6, clearly exceeded 30,000 resolution over the long wavelength portion of the bandpass. The shapes of the long wavelength resolution curves indicate that the resolution is detector limited. At the shorter wavelengths the resolution curves are essentially identical in shape, but substantially lower in absolute resolution and are clearly not detector limited.

Raytrace modeling demonstrates that the LiF channel alignments must be quite good to achieve the detector limited resolution at the long wavelengths. Furthermore, if the resolution at the long wavelengths is detector

limited we should expect the short wavelength resolutions to be detector limited as well. Since we do not see this, the resolution at the shorter wavelengths is probably being limited by something other than defocus, the detector, or grating imaging performance. Another crucial piece of data is that the long wavelength resolution curves were produced using Pt/Ne data and the shorter wavelength resolution curves were produced using H_2 data.

6.2.2 SiC#1 and SiC#2 resolution

While the LiF channels were fairly easy to align, the SiC channels were not. We could never achieve the high resolution values we observed in the long wavelength LiF channels. Using the shotgun method with H_2 spectra we were able to identify the optimum focus of the SiC channels, but the lower absolute values of the resolution, typically around 20,000, concerned us. Finally, we compared the LiF and SiC data globally and found some very interesting patterns.

6.2.3 Comparisons between the SiC and LiF resolution curves

In figure 6 we plot all the resolution curves for all the channels versus wavelength. Immediately apparent is that the absolute value of the resolution decreases significantly as you move towards shorter wavelengths. The decrease is far larger than the expected decrease in resolution due to shorter wavelengths ($\lambda/\Delta\lambda$). Also note that the short wavelength LiF channels cover nearly the same wavelengths as the long wavelength SiC channels and yet the resolutions measured in the

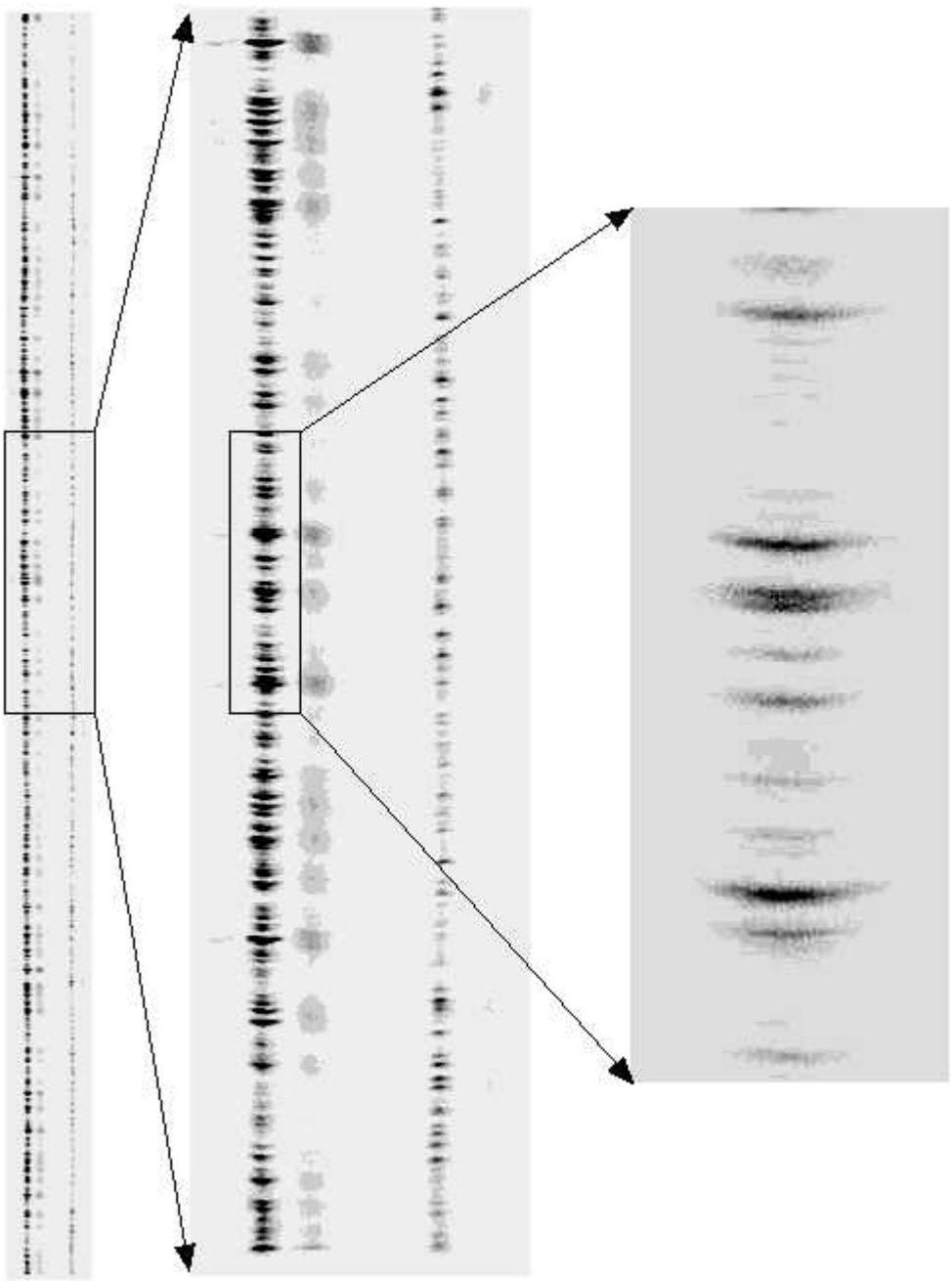

Figure 5: Scaled images of one segment of one flight detector with H/D spectra from the SiC#1 and LiF#1 channels. The left most image is a full detector segment covering approximately 100... The middle is approximately ¬ of the image and then the right most image is 1/16 of the detector segment centered on the LiF spectrum. The LiF spectrum is the spectrum with the largest astimatism... Also evident are the 4 slits and the 30 slits above and below the 1.25 spectra.

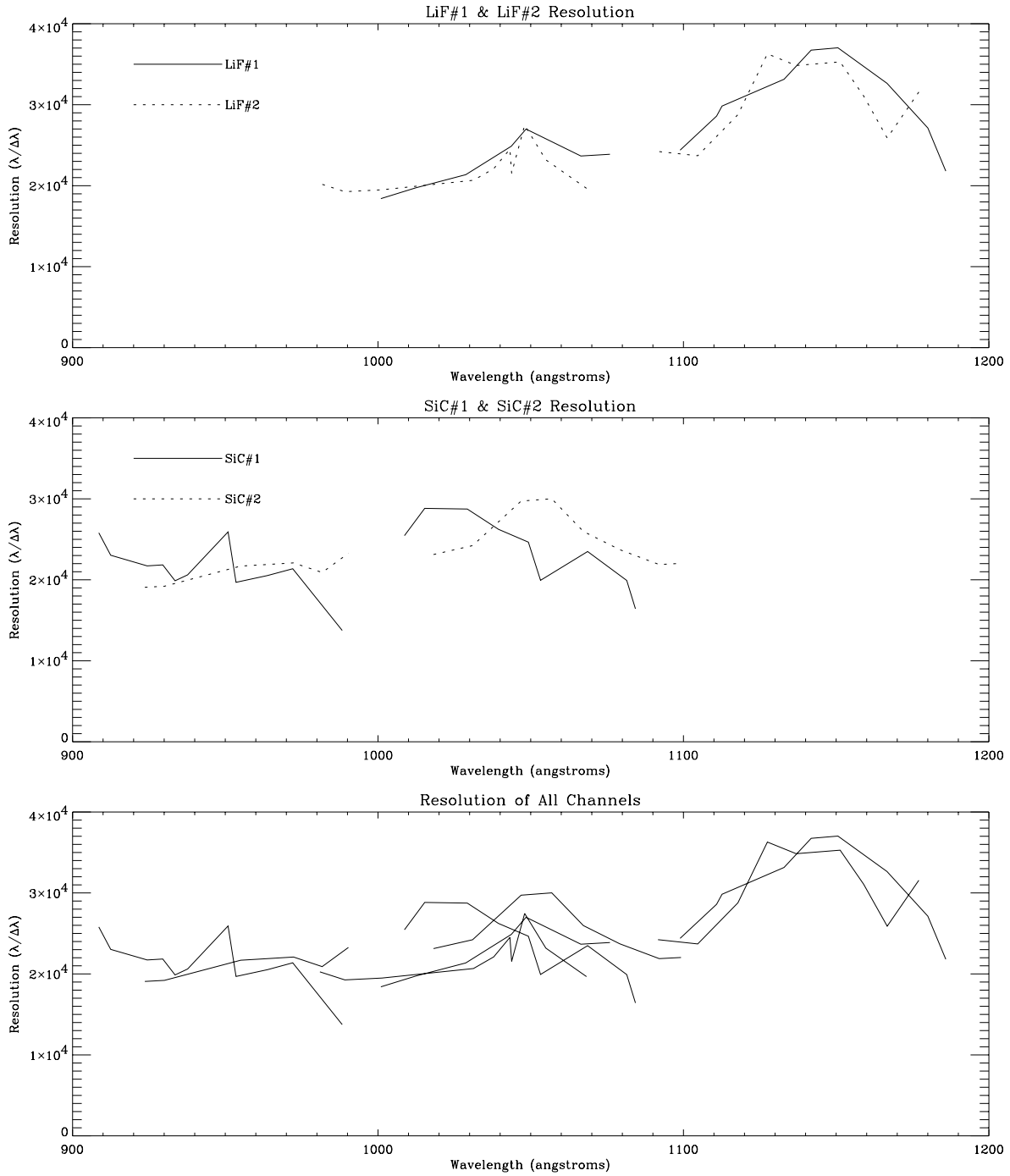

Figure 6: Resolution curves versus wavelengths for the 4 FUVS channels as measured in the laboratory. No corrections for flight performance have been made. Top: Resolution versus wavelength for the LiF#1 and LiF#2 channels. Note that the resolution curves are very similar in both a relative and absolute sense. Middle: Resolution versus wavelength for the SiC#1 and SiC#2 channels. Note that similarity in absolute resolution. Bottom: Resolution curves for all the channels plotted simultaneously. Here it is interesting that the resolution systematically decreases with shorter wavelength.

lab are very similar. It is therefore likely that the H_2 lines being produced by our light sources are not narrow enough to support 30,000 resolution and that any resolution measured in the laboratory with H_2 can be considered a lower limit.

6.3 Efficiency

The end-to-end efficiency of the FUVS was never directly measured. While it was in our original plan to measure the efficiency of the instrument, schedule constraints made this measurement impossible. However, the component level testing at delivery found that the individual component efficiencies met or exceeded the beginning of life specification. Furthermore, witness sample testing of flight coupons and ground support equipment witness mirrors demonstrated that there were no significant contamination events during the processing of the FUVS, so there is no reason to believe the instrument suffered a significant drop in efficiency. Finally, the LiF channels show. observable. efficiency. far. below. the. LiF. cut-off. at. 1050.... This. would. only. be. possible. if. the. LiF. was. in excellent condition.

6.3.1 Contamination control and monitoring

The contamination requirements of the FUSE mission placed stringent requirements on contamination control and monitoring of the flight optics. The contamination requirements imposed on the instrument were similar to those imposed on the Hubble Space Telescope UV instruments. In order to provide sufficient safety and monitoring a variety of techniques were used to track contamination in and out of the vacuum environment.

Our primary line of defense in contamination control during non vacuum operations was to maintain the UV optics on a continuous dry nitrogen purge from a centralized LN2 boil off system. Our main concern was exposure of the LiF coatings to humidity, which can very quickly degrade the reflectivity of Al/LiF. Once installed onto the structure the flight gratings were only exposed during the pump out of the vacuum chamber. The grating saw no more than 50 hours of exposure to room air with <30% relative humidity during component level testing and integration and test. This exposure is below the exposure budgets developed to protect the LiF coatings.

During all vacuum operations involving the flight hardware one to three temperature controlled quartz crystal microbalance (TQCM) were in used to monitor contamination deposition rates. In general the rates observed during integration and test were between 5-20 Hz/hr at -20°C. A residual gas analyzer (RGA) was used to track the types of material present in the chamber during vacuum operations. Non volatile residue (NVR) collection plates were also installed at the beginning of each vacuum cycle. Finally, flight and GSE witness mirrors were installed at various locations within the vacuum chamber as a direct measurement of optical degradation due to contamination. These samples were measured at numerous times throughout integration and test. At no time during integration did we experience any contamination event which could be expected to drastically decrease the efficiency of the instrument.

6.4 Scattered light

There are two sources of scattered light which can compromise the instruments sensitivity, in band scatter from the grating itself and out of band scatter from surfaces such as the internal spectrograph baffles or other illuminated surfaces within the spectrograph cavity. The in band, grating scatter was measured at the component level to be 1 X 10^{-5}/.... This. is. a. typical. scattering. number. for. holographically. ruled. gratings... The. out. of. band scatter is much more difficult to measure
due to the wide dynamic range between the input light and the scattered light required. The aggressive development schedule for the FUVS precluded a precise measurement and characterization of the scattered light in the FUVS. Instead we chose to make an acceptance test measurement which we felt would tell us the approximate limit.

The out of band scattering limit was determined through scaling arguments which enabled us to determine the incident flux of 1216 into the instrument. A MgF2 window was used to eliminate all light below 1150 so that the detector would not be damaged by the remaining 30 of in band light. We then measured the count rates on the detectors and examined the data for any sign of glints or structure in the scattered light. The scattered light from the 1216 produces a fairly uniform background across the detector with a general trend of lower count rates at the shorter wavelengths. No glints or large scale structure which could complicate the data analysis are evident. Through scaling arguments we calculate a scattering efficiency upper limit of approximately 1×10^{-4}/. Our calculations show that this amount of scatter should not adversely effect the scientific performance of the instrument.

6.5 Stability testing

6.5.1 Vibration testing

In the original integration and test plan of the FUVS was to be aligned, all components staked for flight, and then undergo vibration testing, be tested again with FUV light, and then delivered to JHU. However, due to scheduling and risk issues that arose during the integration of the instrument we chose to vibrate the RC1 side of the instrument and employ mass models on the RC2 side. The instrument was successfully shaken in December 1997. Post shake theodolite metrology measurements found no measurable change in the rotational and translational alignments of the optical components and FUV testing found no appreciable degradation in the instrument performance.

6.5.2 Thermal distortion test

Each GMA was designed to operate between 17 and 27øC. To test this capability we used the flight heaters on the GMA thermal enclosure to warm up SiC#1 GMA from 20øC to 28øC over a 4 hour period. During that time we monitored the resolution of the instrument. The GMA performance was unchanged until the grating reached at temperature of 28øC , at which point significant degradation of the data became apparent.

6.5.3 Detector induced effects

Towards the end of FUV integration and test we became aware of certain detector induced effects which are currently under study. The stability of the detector image depends upon the thermal environment of the detector head and the support electronics. The support electronics are located in a far less stable thermal environment that the detector head. To characterize these effects spectral images and stim pulse data were acquired versus temperature to produce a data set which will aid in deconvolving the thermal drift of the detector during flight observations. Stim pulses are generated within the detector to simulate real events from the MCP stacks. Therefore, any change in the performance of the detector electronics can be tracked by monitoring the stim pulses. Flat fields were also acquired as a function of temperature to help understand how to deconvolve the fixed pattern noise of the detector in flight.

7. CONCLUSIONS

On February 16, 1998 the University of Colorado s Center for Astrophysics and Space Astronomy delivered to the Johns Hopkins University the Far Ultraviolet Spectrograph, the primary instrument aboard the Far Ultraviolet Spectroscopic Explorer (FUSE). The instrument was assembled and aligned at CASA s Astrophysics Research Laboratory. To the best of our knowledge, as defined by schedule and cost constraints, the FUVS meets or exceeds the performance required to meet the scientific objectives of the FUSE mission.

At delivery much of the characterization data acquired had yet to be analyzed in any systematic or thorough fashion. However, a concerted effort is underway at the Johns Hopkins University to better understand the instrument performance in preparation for flight. Final instrument performance will not be known until after the in-orbit check out and calibration is complete.

8. ACKNOWLEDGEMENTS

This work was supported by Johns Hopkins University under Contract # NAS5-32985. Special thanks go to the entire FUSE team at CASA for their outstanding work in preparing the component and integration and test facilities, especially Gary Kushner. Thanks also to Robert Grange at the Laboratoire Astronomie Spatial, and the entire JHU/FUSE team who camped out in Boulder during the alignment activities, and the University of California at Berkeley team who came often to Boulder to support detector operations.

9. REFERENCES

1. D. J. Sahnow, S. D. Friedman, H. W. Moos, J. C. Green, and O. H. W. Siegmund,. .Preliminary performance estimates for the *Far Ultraviolet Spectroscopic Explorer* (FUSE),.. *SPIE*, vol. 3356, 1998 (this volume).
2. D. J. Sahnow, S. D. Friedman, W. R. Oegerle, H. W. Moos, J. C. Green, and O. H. W. Siegmund,. .Design. and Predicted. Performance. of. the. Far. Ultraviolet. Spectroscopic. Explorer. (FUSE),.. *SPIE*, vol. 2807, pp. 2 – 10, 1996.
3. S.D.. Friedman,. J.C.. Green,. and. E.. Wilkinson,. .Instrument. Description. and. Science. Performance. of. the. Far Ultraviolet. Spectroscopic. Explorer.,. *SPIE*, vol. 2283, pp. 2–11, 1994.
4. J.. C.. Green,. E.. Wilkinson,. and. S.. D.. Friedman,. .The. design. of. the. Far. Ultraviolet. Spectroscopic. Explorer spectrograph.,. *SPIE*, vol. 2283, pp. 12–19, 1994.
5. O. H. W. Siegmund, M. Gummin, J. Stock, G. Naletto, G. Gaines, R. Raffanti, J. Hull, R. Abiad, T. Rodriquez–Bell, T. Magoncelli,. P.. Jelinsky,. W.. Donakowski,. and. K.. Kromer,. .Performance. of. the. double. delay. line. microchannel. plate detectors. for. the. Far. Ultraviolet. Spectroscopic. Explorer,.. *SPIE*. vol. 3114, pp. 283 – 294, 1997.
6. R.. Grange,. .Aberration–reduced. Holographic. Spherical. Gratings. for. Rowland. Circle. Spectrographs,.. Appl.. Opt., vol. 31, pp. 3744–3749, 1992.
7. H.. Noda,. T.. Namioka,. and. M.. Seya,. .Geometric. Theory. of. the. Grating,.. J.. Opt.. Soc.. Am.,. vol.. 64,. pp.. 1031–1048, 1974.
8. J.. Lees,. G.. Allison,. J.. P.. Andrews,. J.. C.. Green,. J.. Westfall,. .Unique. Method. of. Micropositioning. as. Implemented. in the. FUSE. Focal. Plane. Assemblies.,*SPIE*, vol. 3132, pp. 135–145, 1997.
9. A. Shipley,. J.. C.. Green,. J.. P.. Andrews,. E.. Wilkinson,. and. S.N.. Osterman,. .Final. Flight. Grating. Mount. Design. for. the Far. Ultraviolet. Spectroscopic. Explorer.,. *SPIE*, vol. 3132, pp. 98–109, 1997.